Journal of Engineering and Applied Sciences 11 (10): 2255-2263, 2016
ISSN: 1816-949X

Power System Stability Enhancement Including Wind Farm Based Statcom Controller

[1, 2]Issam Griche and [1]Ahmed Gherbia
[1]Department of Electrical Engineering, Faculty of Technologiy, Setif University, Setif, Algeria
[1, 2]Department of Electrical Engineering, Faculty of Engineering, Bouira University, Algeria

Abstract: In this study power system stability enhancement including wind farm based STATCOM controller has been presented. Three controllers have been used; the first lead-lag compensator, the second Proportional-Integral-Derivative (PID) and the third fuzzy logic controller were designed and simulated in this study for controlling a STATCOM at steady of transient analysis. Modeling of different part has been presented in details. The proposed controllers have been validated using a Synchronous Generator (SG) based One-Machine Infinite-Bus (OMIB) system with an integrated Wind Farm (WF) and a STATCOM. Simulation results and comparative study have been carried out. Many contributions have demonstrated in which Fuzzy logic controller present the best performance compered to both other controllers.

Key words: OMIB, WF, transient stability, STATCOM, fuzzy logic, PID, lead-lag compensator

INTRODUCTION

Today, with the current levels of dependence on fossil fuels, the need of reducing the carbon emissions and the prospects of developing, a new innovative technology sector make wind turbine increasingly attractive pushing the world-wide demand for wind energy in electric power systems growing steadily over the last 20 year, especially with the recent reduction in production costs and increase in conversion efficiencies (Hingorani and Gyugyi, 2000).

Wind turbine is a technology that converts the energy kinetic of wind into electricity troughs generator, especially the Squirrel Cage Induction Generator (SCIG). The system with wind turbine has a stability problem, for this reason, to ensure the stability of the power system including wind generator, Flexible AC Transmission System (FACTS) device to improve the stability problem, such as the STATCOM.

Static Compensator (STATCOM) is electronic power shunt Flexible AC Transmission System (FACTS) devices which can control the line voltage at the connection point to the electric power network (Hingorani and Gyugyi, 2000).

In recent years, most papers have suggested various methods for designing STATCOM PID controllers using linear control techniques in which the equations sets were linearized at a specific operating point and the PI controllers were tuned at that point based on the linearized model in order to obtain the best possible performance (Shen and Lehn, 2002; Abido, 2005) and Fuzzy Logic Controllers (FLC) (Chia *et al*., 2004; Ali *et al*., 2007). Among different nonlinear control techniques, methods based on the Neural Network (NN) have been growing into a popular research topic in recent years (Baiyat, 2005; Sahoo *et al*., 2006). Considering the local search ability and low convergence rate, artificial intelligence-based controllers have the potential to overcome the above-mentioned problems (Song and Johns, 1998; Khanmohammadi and Ghaderi, 2007). One such case is the use of expert systems in the given control system. Artificial intelligence techniques have also been used in STATCOM structures, e.g., Neural network controllers (Chandrakar and Kothari, 2007) and Fuzzy Logic Controllers (FLC) (Chia *et al*., 2004; Ali *et al*., 2007).

However, Etingov and Voropai (2006) has proposed Fuzzy PSS (FPSS) design for transient stability improvement; Morris et al have discuss FLC design in AC regulator side of STATCOM (Morris *et al*., 2003). The number of rules that are used in FLC design are a great deal while for each of these FLC different rules have been devised which results in slow response speed of FLC.

The aim of this study is to design, simulate and compare a PID controller, a lead-lag compensator filter and a fuzzy logic controller in STATCOM configuration for transient stability improvement. The designed fuzzy controllers are replaced with the line voltage PID controller, DC link voltage PID controller of the STATCOM.

The proposed STATCOM has been connected to the Point of Common Coupling (PCC) bus for damping oscillations of the studied OMIB system

Coressponding Author: Issam Griche, Department of Electrical Engineering, Faculty of Technologiy, Setif University, Setif, Algeria

including WF. The simulation results illustrate the improvement provided by the proposed fuzzy controllers simultaneous tuning on power system stability.

MATERIALS AND METHODS

The transient generator model: Mathematical models of a synchronous machine vary from elementary classical models to more detailed ones. In the detailed models, transient and subtransient phenomena are considered. Here, the transient models are used to represent the machines in the system, according to following Eq. 1 and 2 (Oudalov, 2003). Stator winding equations:

$$v_q = -r_s i_q - x'_d i_d + E'_q \quad (1)$$

$$v_d = -r_s i_d - x'_q i_q + E'_d \quad (2)$$

Where:

r_s = The stator winding resistance
x'_d = The d-axis transient reactance
x'_q = The q-axis transient reactance
E'_q = The q-axis transient voltage
E'_d = The d-axis transient voltage

Rotor winding (Eq. 3 and 4):

$$T'_{d0}\frac{dE'_q}{dt} + E'_q = E_f - \left(x_d - x'_d\right)i_d \quad (3)$$

$$T'_{q0}\frac{dE'_d}{dt} + E'_d = \left(x_q - x'_q\right)i_q \quad (4)$$

Where:

T'_{d0} = Is the d-axis open circuit transient time constant.
T'_{q0} = Is the q-axis open circuit transient time constant.
E_f = Is the field voltage.

Torque equation:

$$T_{el} = E'_d i_d + E'_q i_q + \left(x'_q - x'_d\right)i_d i_q \quad (5)$$

Rotor equation:

$$2H\frac{d\omega}{dt} = T_{mech} - T_{el} - T_{damp} \quad (6)$$

$$T_{damp} = D\Delta\omega \quad (7)$$

Where:

T_{mech} = The mechanical torque which is constant in this model
T_{el} = The electrical torque

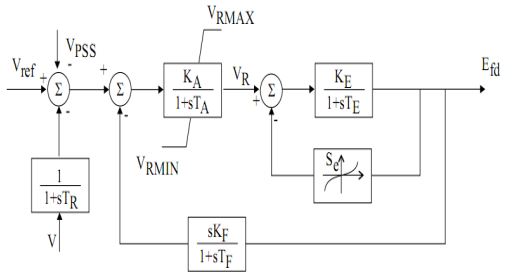

Fig. 1: AVR and exciter model for synchronous generator

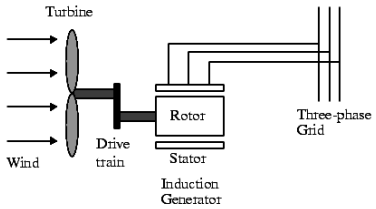

Fig. 2: Grid coupled squirrel cage induction

T_{damp} = The damping torque and is the damping coefficient

For time domain simulation studies, it is necessary to include the effects of the excitation controller. Automatic Voltage Regulators (AVRs) defne the primary voltage regulation of synchronous machines. AVR and exciter model for synchronous generator is modeled as the standard IEEE model (Fig. 1).

Wind turbine model: The Wind Turbine with Induction Generator (WTIG) is shown in Fig. 2. The stator winding is connected directly to the grid and the rotor is driven by the wind turbine. The power captured by the wind turbine is converted into electrical power by the induction generator and is transmitted to the grid by the stator winding.

In order to generate power, the induction generator speed must be slightly above the synchronous speed. The speed variation is typically so small that the WTIG is considered to be a fixed-speed wind generator. The reactive power absorbed by the induction generator is provided by the grid or by some devices such as: capacitor banks. The steady state relation between the wind speed and the aerodynamic power is commonly expressed as:

$$P_v = \frac{\rho \times S \times v_{wind}^3}{2} \quad (8)$$

The stiffness of the drive train is infinite and the friction factor and the inertia of the turbine must be

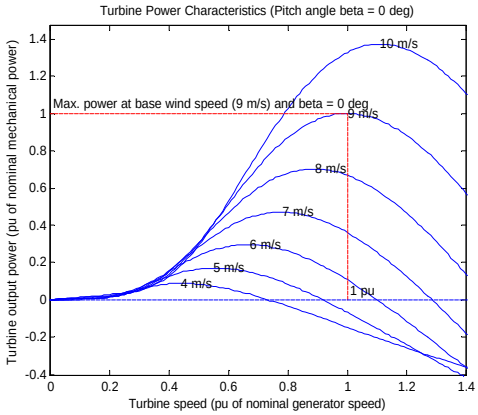

Fig. 3: Turbine power characteristic (b = 0°)

combined with those of the generator coupled to the turbine. Figure 3 illustrates the diagram of wind turbine. The mechanical output power of the turbine or the aerodynamic power appearing to the level of the rotor of the turbine is given by the following Eq. 9:

$$P_{aer} = c_p(\lambda,\beta)\frac{\rho S}{2}v_{wind}^3 \quad (9)$$

Where:
C_p = The performance coefficient of the turbine
ρ = The air density (kg m^{-3})
S = The turbine swept area (m^2)
v_{wind} = The wind speed (m sec^{-1})
λ = The tip speed ratio of the rotor blade tip speed to wind speed
β = Blade pitch angle (deg)

The mechanical power P_{aer} as a function of generator speed, for different wind speeds and for blade pitch angle $\beta = 0°$ is illustrated in Fig. 3. Figure 3 is obtained with the parameters of (base wind speed = 9 m sec^{-1}, maximum power at base wind speed is 1 pu). The tip speed ratio λ is defined as follows:

$$\lambda = \frac{w_h R}{v_{wind}} \quad (10)$$

Where:
W_h = The blade angular
R = The blade length

The drive-train that adapts the speed of the turbine to the speed of the generator is given mathematically in the following Eq. 1:

$$T_g = \frac{T_{aer}}{G} \quad (11)$$

Where:
T_g = The drive-train is torque (Nm)
T_{aer} = The aerodynamic torque (Nm)
G = The drive-train Gain
$\Omega_{turbine}$ = The speed of the turbine (m sec^{-1})
Ω_{mes} = The mechanical speed (m sec^{-1})

$$\Omega_{turbine} = \frac{\Omega_{mec}}{G} \quad (12)$$

Where:
T_g = The drive-train is torque (Nm)
T_{ae} = The aerodynamic torque (Nm)
G = The drive-train gain
Ω_{mes} = The speed of the turbine (m sec^{-1})
Ω_{mes} = The mechanical speed (m sec^{-1})

The mechanical model which considers the inertia total J is given by:

$$J = \frac{J_{turbine}}{G^2} + J_g \quad (13)$$

Where:
$J_{turbine}$ = The inertia of turbine (kg m^{-2})
J_g = The inertia of generator (kg m^{-2})

The evolution of the mechanical speed is:

$$J\frac{d\Omega_{mec}}{dt} = T_{mec} \quad (14)$$

The mechanical torque takes into account the torque electromagnetic, the friction torque and the torque descended of the drive-train given by:

$$T_{mec} = T_g - T_{em} - T_f \quad (15)$$

Where:

$$T_f = f \times \Omega_{mec} \quad (16)$$

where, f is the friction coefficient. The model of Squirrel-Cage Induction Generator (SCIG) is presented by the six coils obey the following electric Eq. 17. For the rotor:

$$v_r = \begin{bmatrix} v_{ra} \\ v_{rb} \\ v_{rc} \end{bmatrix} = \frac{d\phi_r}{dt} + R_r i_r = \frac{d}{dt}\begin{bmatrix} \phi_{ra} \\ \phi_{rb} \\ \phi_{rc} \end{bmatrix} + \begin{bmatrix} R_r & 0 & 0 \\ 0 & R_r & 0 \\ 0 & 0 & R_r \end{bmatrix}\cdot\begin{bmatrix} i_{ra} \\ i_{rb} \\ i_{rc} \end{bmatrix} \quad (17)$$

For the stator:

$$v_s = \begin{bmatrix} v_{sa} \\ v_{sb} \\ v_{sc} \end{bmatrix} = \frac{d\phi_s}{dt} + R_s i_s = \frac{d}{dt}\begin{bmatrix} \phi_{sa} \\ \phi_{sb} \\ \phi_{sc} \end{bmatrix} + \begin{bmatrix} R_s & 0 & 0 \\ 0 & R_s & 0 \\ 0 & 0 & R_s \end{bmatrix}\cdot\begin{bmatrix} i_{sa} \\ i_{sb} \\ i_{sc} \end{bmatrix} \quad (18)$$

The transformation of Park is often defined by the normalized P matrix. The transformation of inverse Park is defined by the P^{-1} matrix. The coefficient $\sqrt{2/3}$ is chosen to give an invariant expression of the electromagnetic torque from the property: $P^{-1} = P$. The system of PARK constitutes a dynamic electric model for the coil two-phase model:

$$v_d = R\times i_d + \frac{d\phi_d}{dt} - \frac{d\theta}{dt}\times\phi_q$$
$$v_q = R\times i_q + \frac{d\phi_q}{dt} + \frac{d\theta}{dt}\times\phi_d \quad (19)$$

$$\begin{bmatrix} v_{sd} \\ v_{sq} \end{bmatrix} = \begin{bmatrix} R_s & 0 \\ 0 & R_s \end{bmatrix}\begin{bmatrix} i_{sd} \\ i_{sq} \end{bmatrix} + \frac{d}{dt}\begin{bmatrix} \phi_{sd} \\ \phi_{sq} \end{bmatrix} - \begin{bmatrix} 0 & -\frac{d\theta_s}{dt} \\ \frac{d\theta_s}{dt} & 0 \end{bmatrix}\times\begin{bmatrix} \phi_{sd} \\ \phi_{sq} \end{bmatrix}$$
$$\begin{bmatrix} v_{rd} \\ v_{rq} \end{bmatrix} = \begin{bmatrix} R_r & 0 \\ 0 & R_r \end{bmatrix}\begin{bmatrix} i_{rd} \\ i_{rq} \end{bmatrix} + \frac{d}{dt}\begin{bmatrix} \phi_{rd} \\ \phi_{rq} \end{bmatrix} - \begin{bmatrix} 0 & -\frac{d\theta_r}{dt} \\ \frac{d\theta_r}{dt} & 0 \end{bmatrix}\times\begin{bmatrix} \phi_{rd} \\ \phi_{rq} \end{bmatrix} \quad (20)$$

$$\begin{bmatrix} \phi_{sq} \\ \phi_{rq} \end{bmatrix} = \begin{bmatrix} L_s & M \\ M & L_r \end{bmatrix}\times\begin{bmatrix} i_{sq} \\ i_{rq} \end{bmatrix} \quad (21)$$
$$\begin{bmatrix} \phi_{sd} \\ \phi_{rd} \end{bmatrix} = \begin{bmatrix} L_s & M \\ M & L_r \end{bmatrix}\times\begin{bmatrix} i_{sd} \\ i_{rd} \end{bmatrix}$$

Where:

R_s, R_r, L_s, L_r = The resistances and inductances of the stator and rotor windings is the main inductance

v_{sd}, v_{sq}, v_{rd}, v_{rq}, i_{sd}, i_{sq}, i_{rd}, i_{rq}, φ_{sd}, φ_{sq}, φ_{rd}, φ_{rq} = The d and q-components of the space phases of the stator and rotor voltages, currents and flux

The torque electromagnetic is given by this expression:

$$T_{em} = p(\phi_{sd} i_{sq} - \phi_{sq} i_{sd}) \quad (22)$$

Or:

$$T_{em} = pM(i_{sq} i_{rd} - i_{sd} i_{rq}) \quad (23)$$

where, p is the number of pair of poles. The equation of the mechanical movement writes:

$$J\frac{d\Omega_{mec}}{dt} = T_{em} - f.\Omega_{mec} - T_r \quad (24)$$

where, T_r is the torque resistance.

Modeling of the statcom: The model of the STATCOM can be written by, respectively:

$$v_{qstat} = V_{dcstat}\times km_{stat}\times\cos(\theta_{pcc} + \alpha_{stat})$$
$$v_{dstat} = V_{dcstat}\times km_{stat}\times\cos(\theta_{pcc} + \alpha_{stat}) \quad (25)$$

Where:

θ_{pcc} = The phase angle of the common AC-bus voltage

V_{dcstat} = The pu DC voltage of the DC capacitor Cm

V_{qsta} and V_{dsta} = The pu q- and d-axis voltages at the output terminals of the STATCOM, respectively

km_{sta} and α_{sta} = The modulation index and phase angle of the STATCOM, respectively (Wang *et al*., 2009)

Control of statcom: The Routh-Hurwitz MATLAB program was used to check the stability of the system. The state space representation of the plant dynamic as provided was used to confirm that the system is stable, controllable and observable (Fig. 4).

Lead-lag compensator filter design: The standard linear control theory has been employed to control the STATCOM. This approach is based an analog control algorithm using a canonical lead-lag compensator based on a transfer function model. The extension of this method is a state-space-model-based state feedback control technique. This method has also used a linear quadratic index on top of traditional linear state feedback control to achieve optimized performance (Fig. 5).

Design of a pid damping controller for the statcom: This section describes the design procedure and design of the PID damping controller of the proposed STATCOM shown in Fig. 6. The aim of the PID controller for the STATCOM is to achieve stability improvement of the studied SG-based OMIB system with WF based SCIG.

Fuzzy logic control design: The inputs that were in the form of crisp values generated from feedback error (e) and change of error (de) were conditioned in terms of multiplying by constant gains before entering into the

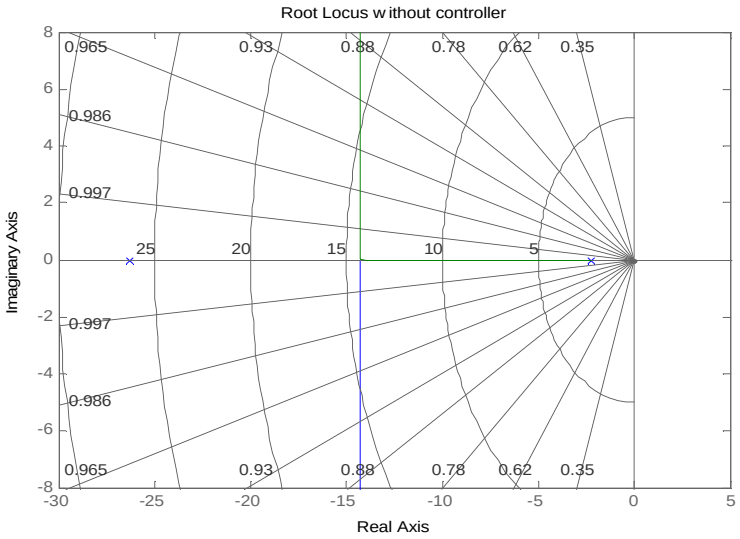

Fig. 4: Root locus plot of the STATCOM with lead compensator

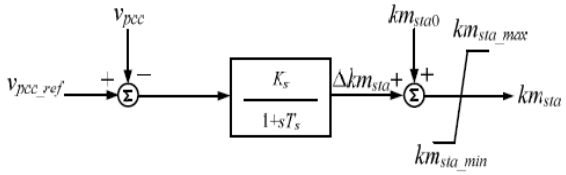

Fig. 5: Control block diagram of the employed STATCOM including the Lead-lag compensator filter

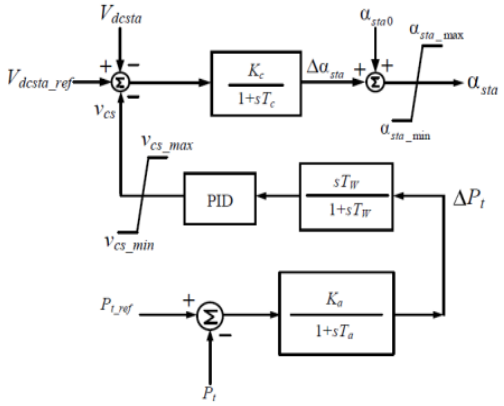

Fig. 6: Control block diagram of the employed STATCOM including the Lead-lag compensator filter

main control block. The fuzzification block converts input data to degrees of membership functions and matches data with conditions of rules. From the rule based

Table 1: Fuzzy logic controller rule table

de/e	NVB	NB	NM	NS	Z	PS	PM	PB	PVB
NVB	PVB	PVB	PVB	PB	PM	PM	PS	Z	Z
NB	PVB	PVB	PB	PM	PS	PS	PS	Z	Z
NM	PVB	PB	PM	PS	PS	Z	Z	Z	
NS	PB	PM	PM	PS	PS	Z	Z	NS	NS
Z	PM	PM	PS	Z	Z	Z	NS	NS	NM
PS	PM	PS	PS	Z	NS	NS	NM	NM	NB
PM	PS	PS	Z	NS	NS	NM	NB	NB	NB
PB	PS	Z	Z	NS	NM	NM	NB	NVB	NVB
PVB	Z	Z	NS	NM	NM	NB	NB	NVB	NVB

Table 2: Performance of controllers to step input

Controller	Rise time (sec)	Overhout	Setting time (sec)	Peak amplitude	Final value
Lead compensator	0.0840	0.00	0.194	0.911	0.911
Final lead lag compensator	0.0798	3.27	0.434	1.030	0.999
PID contol	0.0452	4.40	0.328	1.040	1.000
Fuzzy logic	0.0543	11.4	0.572	1.210	1.000

commands, the Mamdani-type inference engine determined the capability of degree of employed rules and returned a fuzzy set for defuzzification block where the fuzzy output data were taken and crisp values were returned. The outputs of the fuzzy sets were converted to crisp values through centroid defuzzification method. The post processing block then converted these crisp values into standard control signals. In this project, experiential knowledge was borrowed from proportional integral control error and change of error to define fuzzy membership functions. The rule Table 1 was then designed and used with a triangular membership function inputs-output in the fuzzy logic controller and was implemented in the simulation (Table 2).

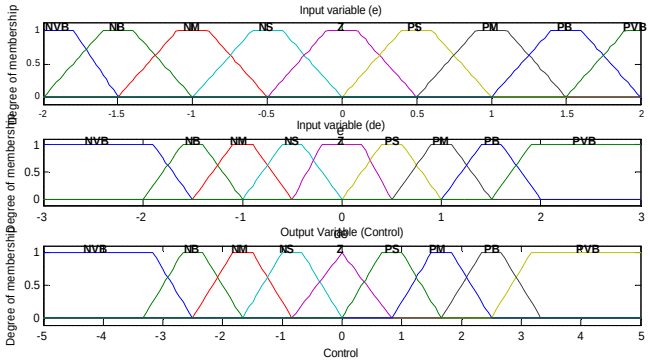

Fig. 7: Fuzzy logic, error, change of error and control

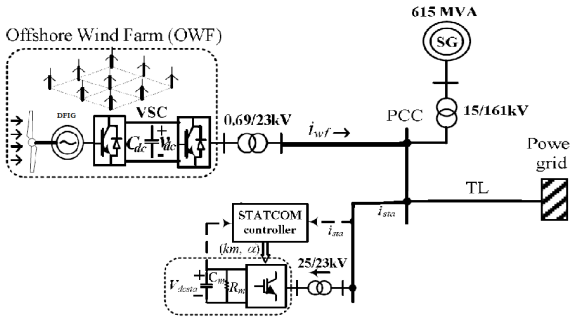

Fig. 8: Case studied

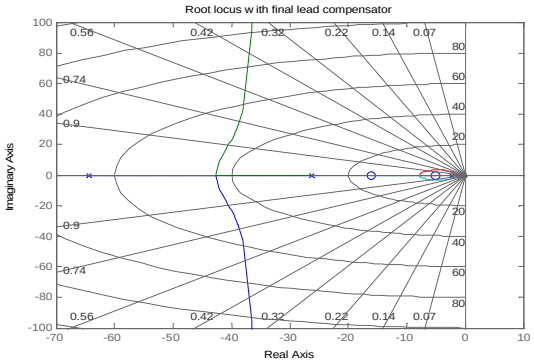

Fig. 9: Root locus of the STATCOM with final lead-lag compensator

RESULTS AND DISCUSSION

These rules make control efforts based on several if then statements about (e) and (de), i.e., if the error is equal Negative Big (NB) and change of error is equal to Negative Medium (NM), then the change in Control (c) is Positive Big (PB). The numbers of these if-then statements were determined based on experiment and tuning of the system. Plots of fuzzy logic membership function for the two inputs variables (e) and (de) and the output (c) are shown in Fig. 7.

Figure 8 show the configuration of the studied SG-based OMIB system containing the integrated wind farm based withSCIG -based WF with a ± 50-MVAR STATCOM. The root locus plots of the system with final lead-lag and PID controller designs are also shown in Fig. 9 and 10 respectively which proves that the design criteria with the desired poles locations have been satisfied. The system responses and control signals are provided for the three controller design in Fig. 11. For the step and sinusoidal input which simulates the STATCOM, the fuzzy logic controller produces

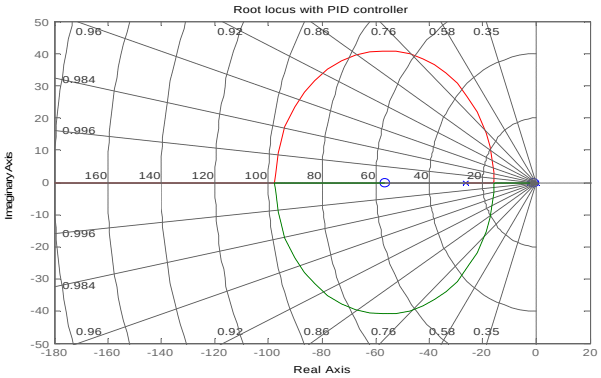

Fig. 10: Root locus of the Statcom with PID controller

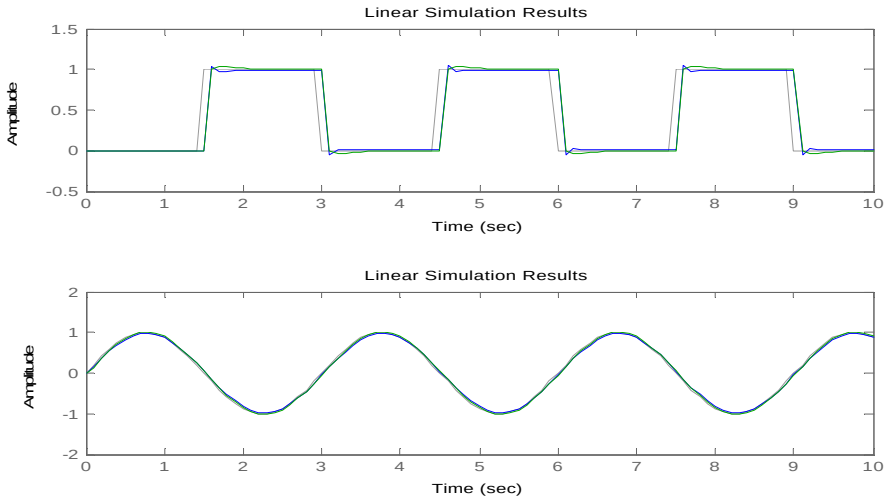

Fig. 11: Plot of control signal for the three controllers for sinusoidal and step input

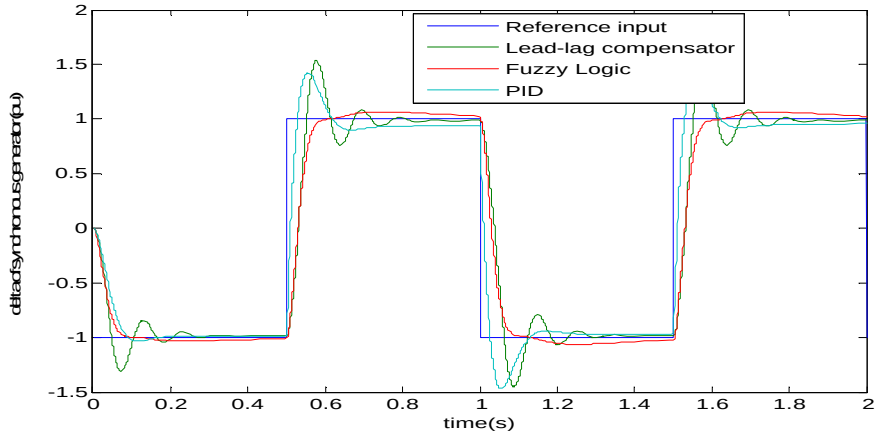

Fig. 12: Transient responses of the studied system with the designed STATCOM and three controllers (rotor angle of SG)

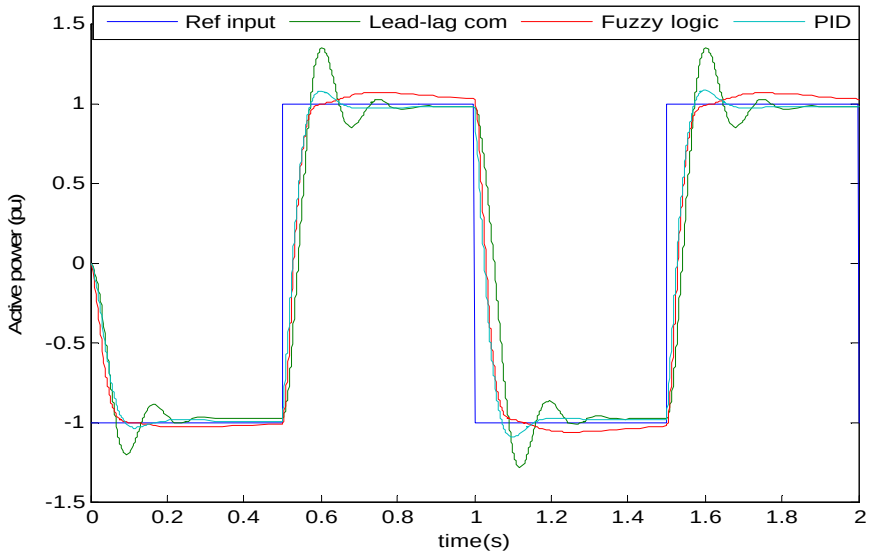

Fig. 13: Transient responses of the studied system with the designed STATCOM and three controllers (active power at PCC)

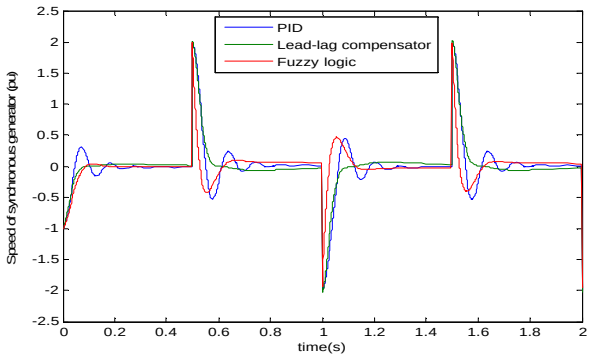

Fig. 14: Transient responses of the studied system with the designed STATCOM and three controllers (Speed of SG)

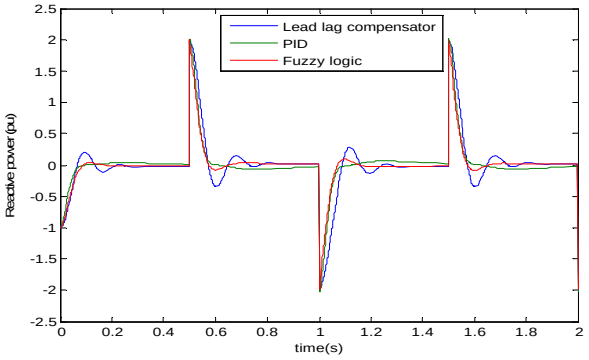

Fig. 15: Transient responses of the studied system with the designed STATCOM and three controllers (reactive power at PCC)

significantly smaller feedback errors. The nonlinear system model developed in to compare the damping characteristics contributed by the proposed STATCOM with the designed three controllers on stability improvement of the studied system. Figure 12-15 plots the comparative transient responses of the studied system, rotor angle of SG, active power at PCC, speed of generator and reactive power at PCC with STATCOM joined with three controllers.

The proposed STATCOM joined with the designed damping controllers stably recovery to the original steady-state operating conditions. It shows that the proposed STATCOM with fuzzy logic controller is a better candidate of the designed damping controller and offer better damping characteristics to quickly damp out the inherent oscillations of the SG-based OMIB system than the PID and lead-lag compensator.

CONCLUSION

This study presents the power system stability enhancement including wind farm based STATCOM controller. A STATCOM design was proposed and connected to the PCC bus. To supply adequate reactive power to the system, three damping controllers for the STATCOM have been designed by the proper controllers

(lead-lag compensator, PID and fuzzy logic controller) to meet the design criteria. Time domain simulations, of the test system subjected to a transient state at the grid have been systematically performed to demonstrate the effectiveness of the proposed STATCOM including with the three damping controllers on suppressing inherent SG oscillations of the studied system and improving system stability.

For the lead-lag compensator design and using root locus, it was found to meet the steady state requirement of the problem. A PID controller was also designed and tuned based on the conventional methods. To achieve smoother control, a fuzzy logic controller with two inputs and one output including 81 rules was also considered.

It can be concluded from the simulation results that the proposed STATCOM with the three damping controllers has the ability to improve the performance of the studied the integrated WF connected to a SG-based power system under transient condition.

REFERENCES

Abido, M.A., 2005. Analysis and assessment of STATCOM-based damping stabilizers for power system stability enhancement. Electric Power Syst. Res., 73: 177-185.

Ali, M.H., T. Murata and J. Tamura, 2007. A fuzzy logic-controlled superconducting magnetic energy storage for transient stability augmentation. IEEE. Trans. Control Syst. Technol., 15: 144-150.

Baiyat, S.A.A., 2005. Power system transient stability enhancement by STATCOM with nonlinear H8 stabilizer. Electric Power Syst. Res., 73: 45-52.

Chandrakar, V.K. and A.G. Kothari, 2007. Comparison of RBFN and fuzzy based STATCOM controllers for transient stability improvement. Proceedings of the International Aegean Conference on Electrical Machines and Power Electronics (ACEMP'07), September 10-12, 2007, IEEE, Nagpur India, ISBN:978-1-4244-0890-0, pp: 520-525.

Chia, B.H., S. Morris and P.K. Dash, 2004. A fuzzy-feedback linearizing nonlinear control of CSI based STATCOM for synchronous generator stabilization. Proceedings of the IEEE International Conference on Control Applications, September 2-4, 2004, IEEE, New York, USA., ISBN:0-7803-8633-7, pp: 1473-1478.

Etingov, P.V. and N.I. Voropai, 2006. Application of fuzzy logic PSS to enhance transient stability in large power systems. Proceedings of the International Conference on Power Electronics, Drives and Energy Systems (PEDES'06), December 12-15, 2006, IEEE, Irkutsk, Russia, ISBN:0-7803-9771-1, pp: 1-9.

Hingorani, N.G. and L. Gyugyi, 2000. Understanding FACTS Concepts and Technology of Flexible AC Transmission Systems. Understanding FACTS Concepts and Technology of Flexible AC Transmission Systems. Piscataway, New Jersey, ISBN:9780780334557, Pages: 432.

Khanmohammadi, S. and O. Ghaderi, 2007. Simultaneous coordinated tuning of fuzzy PSS and fuzzy FACTS device stabilizer for damping power system oscillations in multi-machine power system. Proceedings of the 2007 IEEE Conference on International Fuzzy Systems, July 23-26, 2007, IEEE, Tabriz, Iran, ISBN:1-4244-1209-9, pp: 1-6.

Morris, S., P.K. Dash and K.P. Basu, 2003. A fuzzy variable structure controller for STATCOM. Electric Power Syst. Res., 65: 23-34.

Oudalov, A., 2003. Coordinated control of multiple FACTS devices in an electric power system. PhD Thesis, Ecole Polytechnique Federale de Lausanne, Lausanne, Switzerland.

Sahoo, N.C., R. Ranjan, P.K. Dash and G. Panda, 2006. A novel feedback linearizing STATCOM controller for power system damping. Int. J. Power Energy Syst., 26: 281-290.

Shen, D. and P.W. Lehn, 2002. Modeling, analysis and control of a current source inverter-based STATCOM. IEEE. Trans. Power Delivery, 17: 248-253.

Song, Y.H. and A.T. Johns, 1998. Application of fuzzy logic in power systems, II: Comparison and integration with expert systems, neural networks and genetic algorithms. Power Eng. J., 12: 185-190.

Wang, L., S.S. Chen, W.J. Lee and Z. Chen, 2009. Dynamic stability enhancement and power flow control of a hybrid wind and marine-current farm using SMES. IEEE. Trans. Energy Convers., 24: 626-639.